doi:10.1006/jmbi.2001.4695 available online at http://www.idealibrary.com on IDEAL® *J. Mol. Biol.* (2001) **309**, 961–974

JMB

Ligand-induced Structural Changes to Maltodextrin-Binding Protein as Studied by Solution NMR Spectroscopy

Johan Evenäs, Vitali Tugarinov, Nikolai R. Skrynnikov, Natalie K. Goto Ranjith Muhandiram and Lewis E. Kay*

Protein Engineering Network Centres of Excellence and the Departments of Medical Genetics, Biochemistry, and Chemistry, University of Toronto, Toronto, Ontario Canada M5S 1A8

*Corresponding author

Solution NMR studies on the physiologically relevant ligand-free and maltotriose-bound states of maltodextrin-binding protein (MBP) are presented. Together with existing data on MBP in complex with β-cyclodextrin (non-physiological, inactive ligand), these new results provide valuable information on changes in local structure, dynamics and global fold that occur upon ligand binding to this two-domain protein. By measuring a large number of different one-bond residual dipolar couplings, the domain conformations, critical for biological function, were investigated for all three states of MBP. Structural models of the solution conformation of MBP in a number of different forms were generated from the experimental dipolar coupling data and X-ray crystal structures using a quasi-rigid-body domain orientation algorithm implemented in the structure calculation program CNS. Excellent agreement between relative domain orientations in ligand-free and maltotriose-bound solution conformations and the corresponding crystal structures is observed. These results are in contrast to those obtained for the MBP/β-cyclodextrin complex where the solution state is found to be $\sim 10^\circ$ more closed than the crystalline state. The present study highlights the utility of residual dipolar couplings for orienting protein domains or macromolecules with respect to each other.

Keywords: chemical shift assignment; dipolar couplings; maltodextrin binding protein; protein domains; solution conformation

Introduction

Maltodextrin-binding protein (MBP) belongs to the bacterial superfamily of periplasmic binding proteins[1]. These proteins are involved in the transport of nutrient molecules into Gram negative bacteria and are important for chemotaxis. MBP binds maltodextrins, ($\alpha(1 \rightarrow 4)$-linked glucose polymers), where the number of glucose units ranges from two (maltose) up to seven or eight[2] with affinities in the micromolar range.[3] Maltodextrin-bound MBP interacts with the $MalFGK_2$ protein complex that belongs to the ATP-binding cassette family of transporters. The complex is comprised of the two membrane-associated channel subunits, MalF and MalG, and two copies of a cytoplasmic ATPase, MalK.[4] MBP binding causes ATP hydrolysis by the MalK subunits, leading to active transport of maltodextrin into the cytoplasm.[5] The MBP/maltodextrin complex can also act as a ligand for the Tar receptor.[6] Binding of MBP to the periplasmic domain of Tar leads to a signal transduction cascade in which CheA is dephosphorylated,[7] ultimately resulting in chemotaxis.

X-ray crystallography studies have established that MBP (370 residues, 41 kDa) consists of two globular domains; the N-domain (residues 1-109 and 264-309) and the C-domain (114-258 and 316-370).[1,8] The two domains exhibit similarities in secondary structure and topology, with a central β-sheet flanked on both sides by two or three parallel α-helices. The maltodextrin-binding site is located at the base of a deep groove formed between the two domains. The domain-connecting

Abbreviations used: MBP, maltodextrin-binding protein; DC, dipolar coupling; NOE, nuclear Overhauser enhancement.

E-mail address of the corresponding author: kay@pound.med.utoronto.ca

0022-2836/01/040961–14 $35.00/0

segments, linkers I-III, are comprised of residues 110-113, 259-263 and 310-315, respectively, with the first two linkers forming an antiparallel β-sheet and the third an α-helix. Structures of MBP in complex with physiological ligands show that the binding pocket is lined with a number of polar and aromatic groups from both domains that participate in hydrogen-bonding and van der Waals interactions with the sugar units.[8,9] In the absence of ligand, MBP adopts an open conformation that is related to the closed bound state by a 35° hinge rotation.[10] This type of hinge-bending motion in response to a ligand is believed to be a general feature of periplasmic-binding proteins.[1] Large conformational changes of MBP upon ligand binding have also been demonstrated in solution by thermodynamic, solvent accessibility and small-angle X-ray scattering studies.[11–13] Both Tar and $MalFGK_2$ recognize only the closed conformation of the protein, with the interacting surfaces of MBP formed by residues located in both domains.[14,15] MBP has also been shown to adopt a binding-competent form for both Tar and $MalFGK_2$ when the two domains are brought together in an artificial manner through an inter-domain disulfide bond.[16]

A summary of the five states of MBP for which crystal structures are available is given in Table 1. Although the biological role of MBP involves binding to linear maltodextrins, high-affinity interactions have been observed with non-physiological analogues as well,[17,18] i.e. cyclic maltodextrins or maltodextrins in which the anomeric carbon is oxidized or reduced. Spectroscopic studies indicate that the mode of interaction of these compounds differs from the interactions with physiological maltodextrins.[19–21] In addition, MBP bound to non-physiological ligands does not activate the ATPase or the maltose transporter,[22] seemingly because when bound to these ligands MBP maintains an open conformation.[23] An open conformation has been observed, for example, in the crystal structure of MBP bound to cyclic maltoheptaose (β-cyclodextrin).[24] The bound β-cyclodextrin molecule interacts extensively with the C-domain, while the interactions with the N-domain involve very few direct protein-ligand contacts. Instead, the binding pocket contains many water molecules forming an extensive hydrogen bond network.[24]

Recently, Skrynnikov *et al*.[25] demonstrated that the solution conformation of MBP in complex with β-cyclodextrin is significantly different (~11° more closed) than its X-ray-derived counterpart 1DMB,[24] although the structure of each domain appears to be virtually the same as judged by three-dimensional (3D) models of the solution structure.[26] Here, we expand our studies of MBP to include the physiologically relevant ligand-free (apo) and ligand-bound forms. Chemical shift assignments, $\{^1HN\}$-^{15}N steady-state NOE and residual dipolar coupling (DC) values were obtained for the apo and maltotriose-bound states of the protein using ^{15}N,^{13}C,^2H NMR methodology.[27,28] The chemical shifts establish that the changes in the backbone conformation upon ligand binding are mainly restricted to the interface of the two domains. Long-range structural information on the orientation of inter-nuclear vectors provided by the DC data[29] were used to determine the relative orientation of the two domains in the protein as a function of ligand.[25,30,31] Physically reasonable structural models of the solution conformations of the three states of MBP were generated from DC data and X-ray crystal structures (Table 1) using a quasi-rigid-body domain orientation algorithm implemented in the structure calculation program CNS.[32]

Results and Discussion

NMR studies of the maltotriose-bound and apo states of MBP have been facilitated by recording a series of high quality triple resonance multi-dimensional spectra[33] on ^{15}N, ^{13}C, ^2H-labeled samples. The excellent sensitivity and resolution of ^{15}N-^1HN correlated HSQC spectra recorded on these two states of the protein is apparent from Figure 1. In this regard, we have chosen to work with the maltotriose-bound state and not the maltose-bound form of MBP to avoid the presence of two significantly populated species corresponding to MBP in complex with either the α or β-anomer of the sugar. MBP binds the α-anomer of maltotriose almost exclusively, as the specificity is about 20 times higher when the anomeric (C1) carbon in the reducing end adopts the α-conformation, in contrast to maltose where the α/β anomer specificity ratio is ~2.7.[19] In addition, the β-anomer can be bound in two different modes, probably corre-

Table 1. Information on crystallized states of the maltodextrin-binding protein (MBP)

Ligand state	PDB code	Resolution (Å)	K_D^a (μM)	Closure[b] (deg.)	Twist[b] (deg.)	Bend[b] (deg.)
Ligand-free[10]	1OMP	1.80	-	0	0	0
β-cyclodextrin[24]	1DMB	1.80	1.8	2.8	0.2	−0.4
Maltose[9]	1ANF	1.67	3.5	36.2	−3.5	−2.6
Maltotriose[9]	3MBP	1.70	0.16	34.9	−3.5	−2.9
Maltotetraose[9]	4MBP	1.70	2.3	34.9	−4.1	−3.4

[a] Dissociation constant of the ligand.[3,9].
[b] Closure, twist and bend angles describing the domain orientations are given with respect to 1OMP (see Materials and Methods).

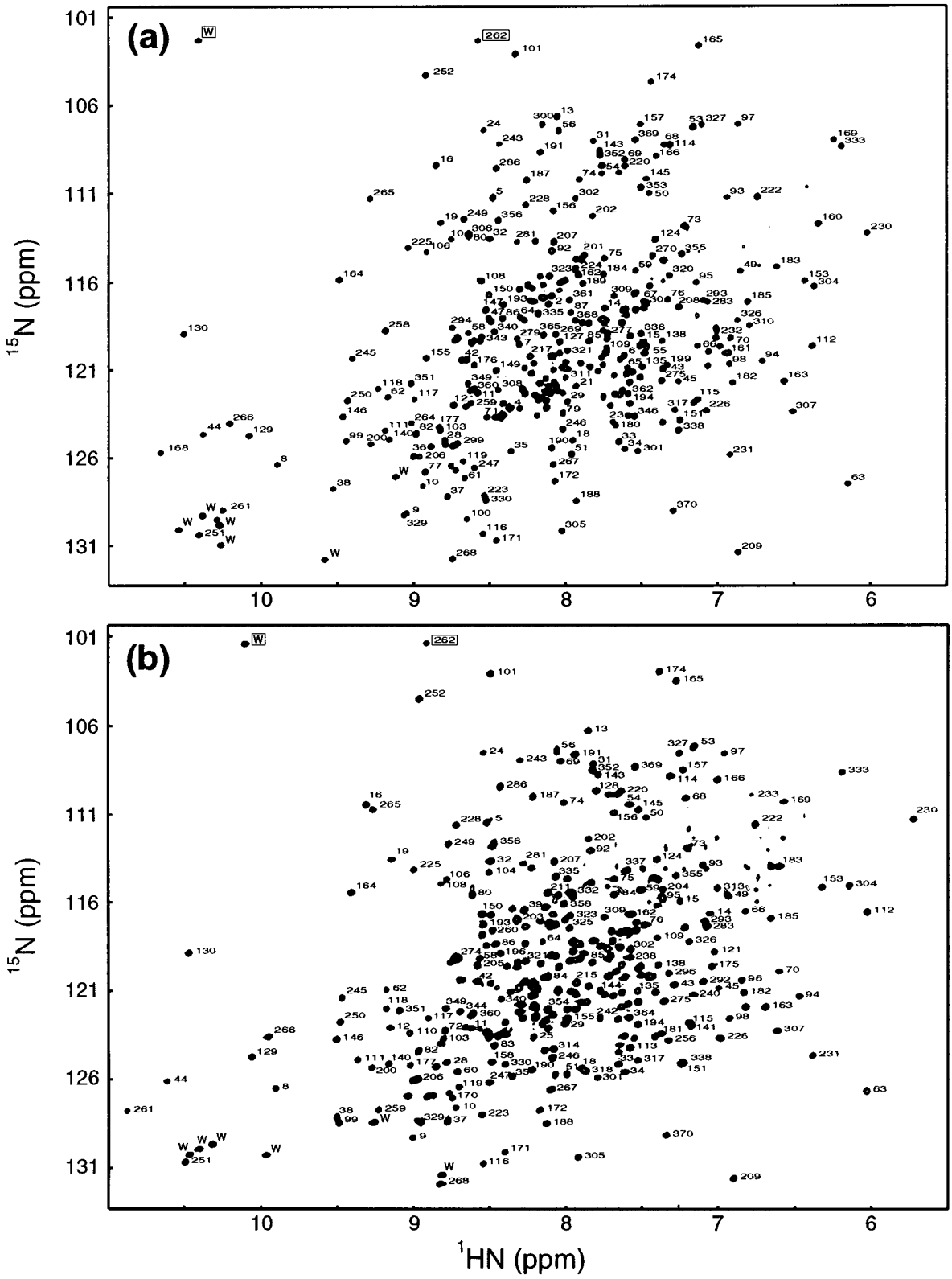

Figure 1. The ^{15}N-^{1}HN TROSY-HSQC spectra[58] of the (a) ligand-free state of MBP and the (b) MBP/maltotriose complex at 37 °C, pH 7.2, 600 MHz. Peaks assigned to backbone amides are labeled by residue number, while those tentatively assigned to Trp side-chain indoles are labeled W. Folded peaks are indicated by a box around the label.

sponding to the closed and open domain conformations of MBP.[19,21,23] In this context it is important to note that only the α-anomer complex has been observed in X-ray structures of MBP with maltose, maltotriose and maltotetraose.[9] Only one set of resonances was observed in the NMR spectra

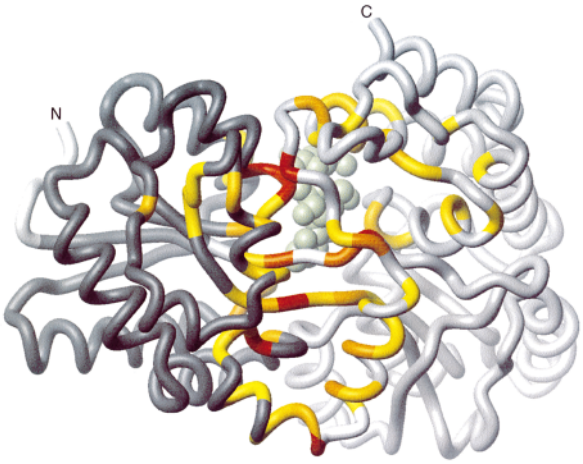

Figure 2. Chemical shift changes in MBP upon binding of maltotriose. The backbone C^{α} trace of the crystal structure of the maltotriose-bound state of maltodextrin-binding protein (PDB entry: 3MBP[9]) is shown. According to the combined chemical shift change,[66] $\Delta\delta_{tot}=\sqrt{(w_N\Delta\delta_N)^2+(w_{C\alpha}\Delta\delta_{C\alpha})^2+(w_{C\beta}\Delta\delta_{C\beta})^2+(w_{CO}\Delta\delta_{CO})^2}$ (w_N=0.154, $w_{C\alpha/C\beta}=0.276$ and $w_{CO}=0.341$), each residue is color-coded from yellow ($\Delta\delta_{tot}=0.2$ ppm) to red ($\Delta\delta_{tot}\geqslant 1.0$ ppm). Otherwise if $\Delta\delta_{tot}\leqslant 0.2$ ppm residues are colored dark gray (N-domain residues 6-109 and 264-309), light gray (C-domain residues 114-258 and 316-370), or white (N terminus and linker residues). A space-filling model of the bound maltotriose ligand is included (pale green). The Figure was generated using MOLMOL.[71]

of the maltotriose state of MBP, indicating that the β-anomer conformer is negligibly populated in the bound state, as expected.

Chemical shift assignments

Near complete (>96 %) assignments of the ^{1}HN, ^{15}N, $^{13}C^{\alpha}$, $^{13}C^{\beta}$ and ^{13}CO chemical shifts of apo-MBP have been obtained. These chemical shifts are remarkably similar to those for the MBP/β-cyclodextrin complex.[34] Pair-wise root-mean-square (r.m.s.) differences of 0.09 and 0.16 ppm are obtained for ^{1}HN and $^{13}C^{\alpha}$ chemical shifts in the apo- and β-cyclodextrin loaded states, for example, with maximal shift changes observed for Y155 (^{1}HN: −1.1 ppm) and I333 ($^{13}C^{\alpha}$: 1.0 ppm). Of interest, assignments were not obtained for residues K1, K83, N173, A186 and S233-N241 in either apo or β-cyclodextrin states.

A near complete assignment of ^{1}HN, ^{15}N, $^{13}C^{\alpha}$, $^{13}C^{\beta}$ and ^{13}CO chemical shifts was obtained for the maltotriose-bound state, with the only missing shifts belonging to residues K1, N100, N173 and N234-N241. Two weak spin systems may tentatively be assigned to S238 and V240 on the basis of the $^{13}C^{\alpha}$ and $^{13}C^{\beta}$ chemical shifts of these residues and those that precede them in sequence (Thr and Lys).[35] X-ray structures of MBP show that residues S233-N241 are part of a helical segment, located at the interface of the two domains of MBP but separated from the maltodextrin-binding site. The absence or weak intensities of cross-peaks for these residues likely reflects conformational exchange and/or fast amide proton exchange with solvent. Since correlations for these residues could not be observed in any of the three studied states of MBP it is unlikely that their absence is linked to ligand binding.

Ligand-induced chemical shift changes in MBP

The assigned backbone and $^{13}C^{\beta}$ chemical shifts have been used as probes of structural changes resulting from ligand binding. Upon binding of maltotriose, substantial chemical shift changes occur for many residues relative to the ligand free state (see Figure 1), with maximum ^{1}HN, ^{15}N, $^{13}C^{\alpha}$, $^{13}C^{\beta}$ and ^{13}CO chemical shift changes of −2.0 (A168), 7.1 (V302), 3.8 (F67), 3.1 (R66) and −2.1 ppm (P298), respectively. Figure 2 displays the combined chemical shift changes (see Materials and Methods) of the heavy nuclei color-coded onto the crystal structure of the maltotriose-bound form of MBP. Ligand-induced changes are observed throughout the primary sequence of MBP, but the effects are clearly spatially concentrated to the domain interface including the maltotriose-binding site and the linker regions. The large backbone and C^{β} chemical shift changes observed for several of the linker residues are consistent with a structural transition involving domain re-orientation upon ligand binding.[10] These results are also in accordance with the crystallographic data, implying that residues in both domains are involved in sugar binding, e.g. D14, K15, E44, W62, D65, R66, E111, E153, Y155, W230, W340 and Y341.[9]

Two distinct conclusions can be reached from comparison of chemical shift changes induced by the physiological ligand, maltotriose, with those induced by the non-physiological ligand, β-cyclodextrin. First, changes in shift are on average two to three times smaller upon binding of β-cyclodextrin. Second, although the changes are smaller, they are in general confined to the same regions in both domains, as illustrated by Figure 3 showing

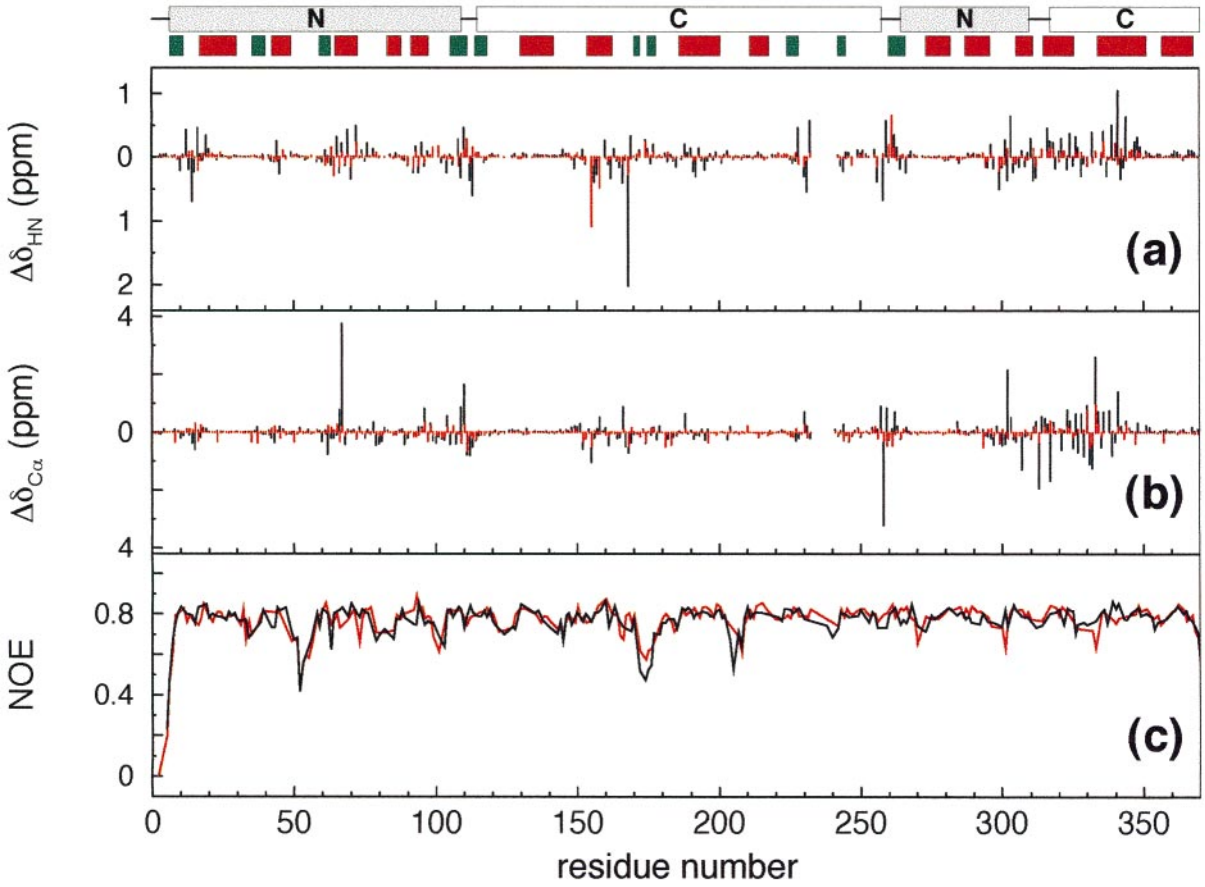

Figure 3. Ligand-induced chemical shift changes and {^{1}HN}-^{15}N steady-state NOE values. The two upper panels show the (a) ^{1}HN and (b) $^{13}C^{\alpha}$ chemical shift changes that occur in MBP upon binding of maltotriose (black bars) and β-cyclodextrin (red bars) as a function of residue. (c) The {^{1}HN}-^{15}N steady-state NOE values monitoring the fast backbone dynamics of the apo (red line) and the maltotriose-bound (black line) states of MBP. Error bars are not displayed for clarity (NOE uncertainties range between 0.01 and 0.06 as estimated from the observed noise level in the NMR spectra). The location of domains and secondary structure is schematically indicated at the top of the figure: N domain (gray), C domain (white), α helix (red), and β strand (green).

the ^{1}HN and $^{13}C^{\alpha}$ chemical shift changes *versus* amino acid sequence. The qualitative similarity of the two ligand-bound states suggests that in solution the N-domain may interact more directly with β-cyclodextrin than what is observed in the crystal structure,[24] where the N-domain mainly contacts the sugar atoms indirectly *via* water molecules with only a few exceptions, K42 and D65. Similarly, despite the fact that the domain orientations in the crystal structure are essentially unchanged upon binding of β-cyclodextrin, we observe changes in chemical shifts for residues in all three linker segments. These data support previous NMR studies showing that the binding of β-cyclodextrin results in a significant domain closure (~14°) relative to the apo-state.[25] This degree of closure would pack the N-domain against the bulky β-cyclodextrin molecule,[25] consistent with the observed chemical shift changes that occur in the N-domain. It remains to be ascertained why smaller shift changes are observed compared to maltotriose binding, in particular for the C-domain where β-cyclodextrin is anchored.

Backbone dynamics on pico- to nanosecond time scales

The {^{1}HN}-^{15}N steady-state nuclear Overhauser enhancement (NOE) values were measured for the apo- and maltotriose states to probe how ligand binding affects protein backbone dynamics. The NOE values indicate that fast backbone dynamics (pico- to nanosecond time scales) are very similar in both these states of MBP (Figure 3(c)). In addition, the values closely match those reported for MBP in complex with β-cyclodextrin.[36] Of course, the similar behavior in all three states does not exclude potential ligand-dependent differences in side-chain dynamics.[37] Overall, the relatively high NOE values suggest that the backbone of MBP is well ordered with a few exceptions, e.g. residues 50-56, 171-176, and 204-208 and amino acids at the termini. A similar trend can be observed from the crystallographic temperature (*B*) factors. Interestingly, two flexible residues (T53 and D55 with NOE values of 0.57 and 0.58, respectively) and one residue near the C terminus

(R367, NOE = 0.78) have been shown to be important for the initial interaction of MBP with Tar.[38] In addition to the fact that the dynamics are unchanged upon ligand binding, the local structure around these residues is also likely preserved, as indicated by minute chemical shift changes. Thus, the recognition by Tar relies on the changes in relative domain orientation that occur upon ligand binding rather than on changes in local structure. Domain closure results in the ''correct'' positioning of T53/D55 in the N-domain and R367 in the C-domain, thereby enhancing the strength of interaction with the periplasmic domain of Tar.

The inter-domain linker segments display little mobility on the pico- to nanosecond time scale, with all NOE values obtained for linker residues larger than 0.70 in all three forms of MBP studied. These results are consistent with the protein tumbling as a rigid body with or without bound ligand, although moderate amplitude inter-domain motion cannot be ruled out on the basis of this data.

Dipolar couplings have been measured for the three states of MBP

Domain orientation in MBP has been investigated using the long-range structural information available from residual dipolar couplings (DC).[29,39] The DC values, measured from fractionally aligned molecules dissolved in a dilute solution of aligning media, strongly depend on the orientation of dipolar vectors relative to the molecular alignment frame, *cf.* equation (2) in Materials and Methods. Using Pf1 phage,[40] an appropriate degree of alignment of MBP was achieved with little decrease in spectral quality. In the present study, one-bond ^{1}HN-^{15}N, ^{15}N-^{13}CO and ^{13}CO-^{13}C$^{\alpha}$ DC data ($^{1}D_{NH}$, $^{1}D_{NCO}$, $^{1}D_{COC\alpha}$) were used. Similar DC data sets have been recorded for the MBP/β-cyclodextrin complex.[41] In addition, a set of $^{1}D_{C\alpha C\beta}$ values was included in the analysis of the apo state.[42]

Of note, we have observed that when the experimental dipolar coupling values are compared to those predicted on the basis of X-ray structures, *cf.* equation (2), the $^{1}D_{NCO}$ and $^{1}D_{COC\alpha}$ couplings generally show equal or slightly better agreement with the predicted couplings than do the $^{1}D_{NH}$ values, despite the fact that the ^{1}HN-^{15}N couplings are of increased precision.[41] One possibility is that the order parameters of the ^{1}HN-^{15}N bonds vary more than do those for the bonds connecting two heavy nuclei. If this is the case the prediction of $^{1}D_{NH}$ values would be less accurate, since a uniform value of the order parameter is assumed in the calculations. However, we have not observed a correlation between dynamics parameters obtained from spin relaxation studies and deviations between predicted and measured DC values. More likely potential sources of error are non-uniformity of HN-N bond lengths due to hydrogen bonding and deviations from assumed planarity of the peptide unit.

Solution conformations of MBP

In the present study we have used DC data to obtain the relative orientation of domains in MBP as a function of a number of different ligands. Domain orientation in a given structure is described in terms of three rotations about the so-called closure, twist and bend axes[25,43] (in that order) that are required to transform the 1OMP X-ray structure[10] to the structure in question. Rotations about these three axes are equivalent to a single rotation about an effective hinge axis.[10,25,44] Details of the closure, twist and bend axis system have been described previously.[25] Briefly, the twist axis is defined by the unit vector parallel to the line connecting the centers of mass of the N and C-domains in the 1OMP X-ray structure. The closure axis is derived from the hinge axis about which the rotation is performed to transform the open 1OMP structure into the closed 1ANF structure, with the closure axis given by the component of this hinge axis that is orthogonal to the twist axis. The bend axis is defined by the cross product of the unit vectors along the twist and closure axes. The same set of axes has been used for all analyses, with the PDB frame of the 1OMP structure[10] serving as the reference frame, i.e. the closure, twist and bend angles describing the 1OMP conformation are {0°, 0°, 0°}.

Structural models of the solution conformations of MBP with relative domain orientations that agree with the experimental dipolar couplings were generated from X-ray crystal structures. To reduce the discrepancies between experimental and predicted DC values due to dynamic and/or static disorder, DC values reporting on bond vectors in ill-defined regions of the X-ray structures were removed. Data were excluded on the basis of the crystallographic *B*-factors as described in Materials and Methods. Following the exclusions, 959, 725 and 818 DC restraints for apo, β-cyclodextrin, and maltotriose-MBP, respectively, were employed in the analyses.

To produce physically reasonable structural models of MBP, domain rotations were performed using a quasi-rigid-body refinement protocol involving low temperature torsion angle simulated annealing implemented in the structure calculation program CNS[32] (see Materials and Methods). This approach was very recently employed in solution studies of phage T4 lysozyme.[45] The rationale for a rigid-body approach is that the intra-domain structure of MBP appears quite insensitive to the presence of ligand, i.e. the pair-wise backbone r.m.s.d. for the N and C-domains range between 0.2-0.4 and 0.2-0.7 Å, respectively, for the X-ray structures given in Table 1. Furthermore, chemical shift analyses indicate that the secondary structure of each domain is the same in solution and X-ray states. In addition, the domain structure of MBP in complex with β-cyclodextrin has recently been shown to be essentially identical in the solution and crystal forms of the molecule.[26] Finally, DC data from the

ligand-free as well as the maltotriose-bound state, as analyzed on a per domain basis, are in good agreement with values predicted from the X-ray structures as established using the program Conformist 1.0.[25]

To preserve the intra-domain backbone structure in the CNS calculations, a large number of tight distance and dihedral angle restraints were generated for each domain from the respective X-ray structures (see Table 1). Thus, each domain was treated in the structure calculations essentially as a rigid body, with the relative domain orientation adjusted according to the set of experimental DC-based restraints. Synthetic restraints were limited to intra-domain distances and dihedral angles with experimental DC restraints included for each domain and the linker regions. Restraints were not included for side-chains so that various conformations could be more easily accommodated without steric clashes.[46] Using this protocol, ten structural models were calculated starting from each of the five crystal structures listed in Table 1. Thus, 50 models were obtained for each of the three solution states of MBP studied.

The results from this approach are illustrated in Figures 4 and 5. Figure 4 shows schematically the domain orientations observed in solution (b) as compared to those found in the crystal structures (a). The indicated closure, twist and bend values for solution conformations are calculated by averaging over ten models for each of the five starting X-ray structures. Variations in the closure, twist and bend angles obtained in this manner are due, in large part, to structural noise, illustrated by the differences in positions of each sphere in a set of five like-colored spheres, where each of the spheres corresponds to a different starting X-ray structure. In addition, within each set of ten structures calculated from a given starting X-ray conformation there was a significant spread in twist in one or two cases (by as much as 8°). Mean values and standard deviations of closure, twist and bend angles for all 50 calculated CNS structural models are given in Table 2, along with the alignment parameters for each solution state of MBP investigated.

Well-defined solution conformations were obtained for each of the three states of MBP studied (Table 2 and Figure 4). Only very small differences are observed between NMR and X-ray (1OMP) derived models of the apo state in terms of relative domain orientations (*cf.* Tables 1 and 2). Even better agreement is achieved for the maltotriose-bound state of MBP, i.e. closure, twist, bend values of {34.9(±0.7)°, −3.0(±1.5)°, −2.2(±1.1)°} in solution *versus* {34.9°, −3.5°, −2.9°} in the crystal (3MBP[9]). These results clearly indicate that relative domain orientations observed in crystal and solution states can be very similar, thus providing an important benchmark for domain orientation studies by NMR. The results for the apo and maltotriose-bound states are in strong contrast to those

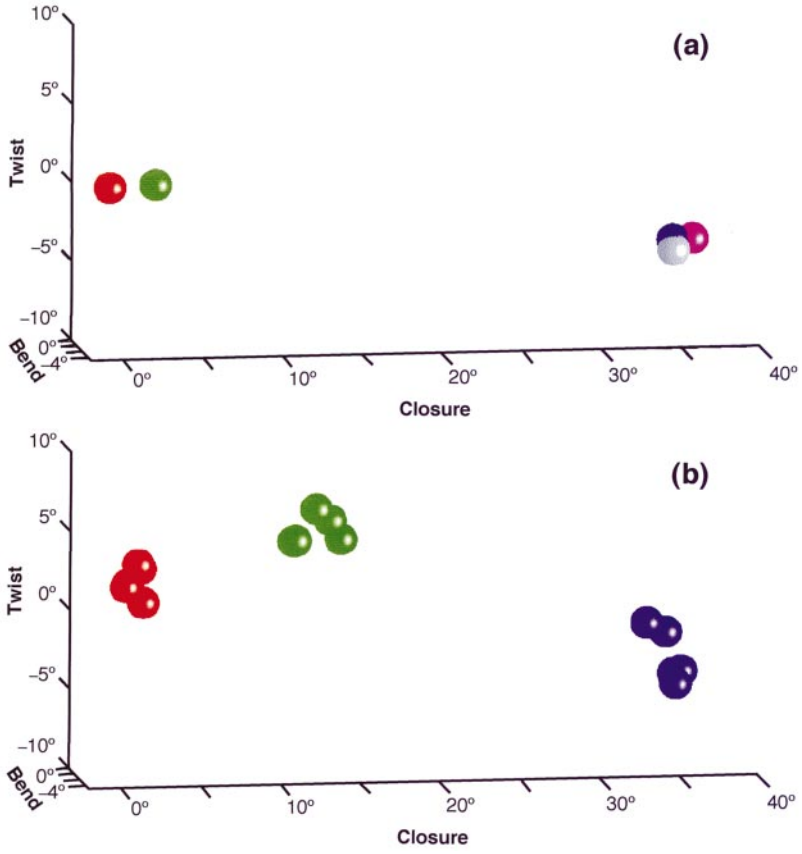

Figure 4. Schematic representation of the relative orientation of the N and C-domains in different states of MBP as studied by (a) X-ray crystallography and (b) NMR spectroscopy. (a) The spheres represent different X-ray crystal structures, 1OMP, 1DMB, 1ANF, 3MBP, and 4MBP, that correspond to the apo (red), β-cyclodextrin (green), maltose (magenta), maltotriose (blue) and maltotetraose (gray) states, respectively. All angles are referenced relative to the 1OMP structure, *via* three sequential orthogonal rotations (closure, twist and bend) as outlined in Materials and Methods. (b) Each sphere represents the solution conformation obtained using the DC data of the apo (red), β-cyclodextrin-bound (green), and maltotriose-bound (blue) states, respectively. For each solution state studied, five balls are displayed with each ball corresponding to the mean of ten solution conformations derived from one of the five X-ray crystal structures shown in (a), as described in the text.

Table 2. Alignment parameters and solution conformations of MBP

Ligand state	$A_a/10^{-3}$[a]	R[a]	α, β, γ[a,b] (deg.)	Closure[c] (deg.)	Twist[c] (deg.)	Bend[c] (deg.)
Ligand-free	1.48 ± 0.01	0.25 ± 0.01	98,28,43	1.3 ± 0.6	2.4 ± 1.9	−2.2 ± 0.8
β-cyclodextrin	1.52 ± 0.01	0.18 ± 0.01	78,31,50	12.8 ± 1.3	5.3 ± 2.3	−1.3 ± 0.9
Maltotriose	1.49 ± 0.01	0.42 ± 0.01	57,45,51	34.9 ± 0.7	−3.0 ± 1.5	−2.2 ± 1.1

[a] Alignment parameters, see equation (2), are calculated by direct fitting of the DC data to each of the calculated CNS structures. The error denotes the standard deviation calculated from the 50 CNS structures.
[b] Euler angles {α,β,γ} describe the orientation of the alignment tensor with respect to the molecular frame of the 1OMP crystal structure. Standard deviations range from 1° to 2°.
[c] Closure, twist and bend angles of the domains are given with respect to the 1OMP crystal structure (see Materials and Methods). The error denotes the standard deviation calculated from the 50 CNS structures.

from domain orientation studies of the MBP/β-cyclodextrin complex where the solution and crystalline states are noticeably different. Using the CNS-based approach the solution structure is found to be 10° more closed, in good agreement with previously reported results.[25]

Very recently Hwang *et al.*[36] confirmed the domain closure in the β-cyclodextrin-loaded MBP state by calculating rotational diffusion tensors for the two domains of MBP using backbone ^{15}N T_1 and $T_{1\rho}$ relaxation rates[47] measured in the isotropic solution phase. Similar analyses of ^{15}N spin relaxation data of apo-MBP also agree with the observed open solution conformation obtained here (data not shown). Thus, the discrepancy observed for the β-cyclodextrin/MBP complex should be attributed to differences between the solution conditions and the crystalline environment.

Crystal packing interactions have been shown to alter the relative domain positioning of other members of the superfamily of periplasmic binding proteins.[48,49] Interestingly, isomorphous crystals used for X-ray studies often lead to similar relative domain orientations, as can be seen from the X-ray crystallographic studies of lysozyme mutants.[50] In this context it is noteworthy that the crystals of the MBP/β-cyclodextrin complex were grown under similar buffer conditions as those of the ligand-free state and that both these states crystallized in the same space group *P*1.[24] Presumably, crystal packing stabilizes one conformation from the range of conformers which are potentially accessible to MBP in solution and this particular crystal state happens to be significantly more open than the average solution conformation.

Backbone representations of the solution conformations of the different states of MBP illustrating changes in relative domain orientations upon ligand binding are shown in Figure 5. An important benefit of the CNS-based approach relative to the previous methods we have employed where individual domains were rotated independently[25] is that not only are relative domain orientations obtained but so too are physically reasonable relative positions of the domains.[45] In this way, we obtain a complete picture of the average solution

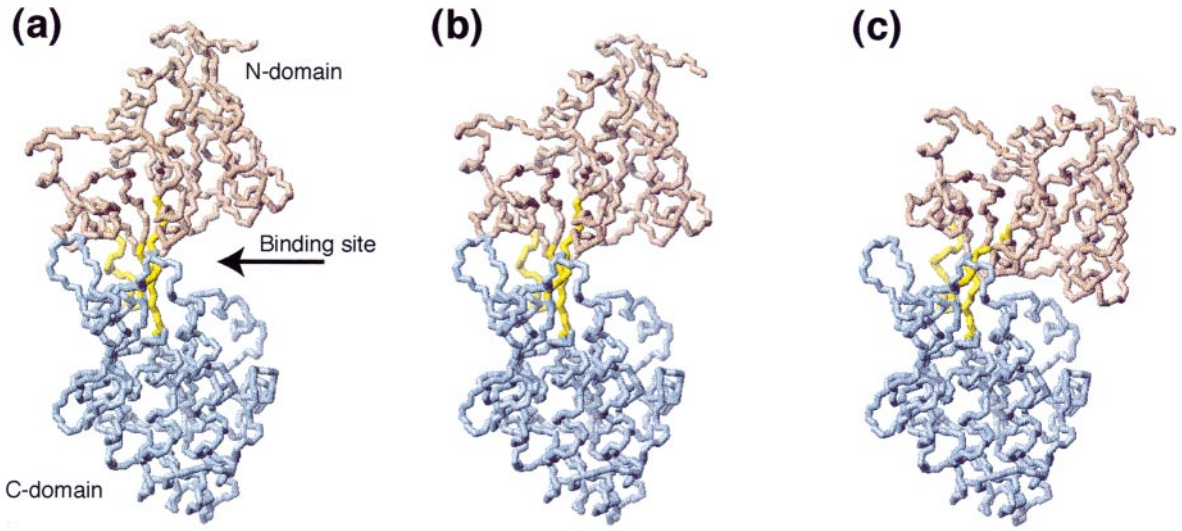

Figure 5. Structural models of the solution conformations of MBP. Backbone representations of the models are shown for the (a) apo state, (b) the β-cyclodextrin-bound state and the (c) maltotriose-bound state of MBP with the C-domain (114-258, 316-370) of each structure aligned. The Figure is produced so that the horizontal and vertical axes correspond to the bend and twist axes, respectively. The perpendicular closure axis is pointing into the plane of the Figure. The N and C-domains are colored red and blue, respectively, while the linker region is shown in yellow. The maltodextrin-binding site is located in the cleft formed between the domains (indicated by an arrow in (a)). The Figure was generated using MOLMOL.[71]

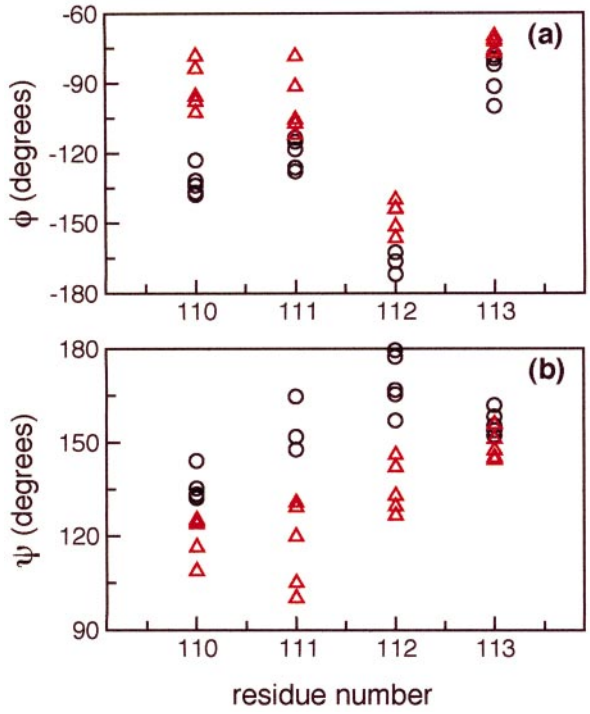

Figure 6. Analysis of the backbone conformation of linker I (V110-L113). The values of the dihedral angles (a) ϕ and (b) ψ are shown for the solution conformations of ligand-free (red triangles) and maltotriose-bound (black circles) MBP. Five values are shown for each residue each representing the average angle of 10 CNS models derived from the same X-ray structure.

conformation, including the structure of the linker regions connecting the two domains. All three of the linkers are involved in the conformational changes associated with domain closure. A comparison of ϕ and ψ dihedral angles obtained from the closed maltotriose-bound and open ligand-free solution structures of MBP shows that domain closure involves small changes that are distributed over several successive residues. No single ''hinge'' residue, responsible for an abrupt change in the direction of the protein backbone can be identified in any of the linker segments. The ϕ and ψ angles of linker I (V110-L113) are slightly but systematically shifted between the two states, as shown in Figure 6. A similar range of ϕ and ψ changes were observed for linkers II (V259-S263) and III (E310-P315), although no systematic trends were noted.

The quality of the CNS structures calculated as described above was assessed using PROCHECK.[51] Bond lengths, bond angles, planarity of peptide bonds and the backbone dihedral angles ϕ and ψ were found to be at least as good as those of the starting X-ray structures. A heavy backbone atom pair-wise r.m.s.d. values between initial X-ray and calculated CNS structures was on average 0.03(±0.01) Å on a per domain basis, implying essentially unchanged domain backbones (the corresponding r.m.s.d. values for heavy-atoms in side-chains are in most cases >1 Å). The good covalent geometry and the close similarity with the initial X-ray template indicate that the structures of the domains are not distorted in order to satisfy the DC restraints.

The compatibility between the DC sets and the calculated CNS structures was established by calculating quality (Q) factors:

$$Q = \sqrt{\frac{\sum_{i=1,N} (D_i^{\text{meas}} - D_i^{\text{calc}})^2}{\sum_{i=1,N} (D_i^{\text{meas}})^2}} \qquad (1)$$

The Q factor provides a way of assessing the agreement between experimental DC values and those predicted from a 3D structure that is independent of the degree of alignment.[52] Q values ranging between 0.09 and 0.22 were obtained for any DC set, $^1D_{\text{NH}}$, $^1D_{\text{NCO}}$, $^1D_{\text{COC}\alpha}$ or $^1D_{\text{C}\alpha\text{C}\beta}$. Of note, the DC values predicted on a per domain basis from the 1DMB crystal structure[24] (β-cyclodextrin-MBP) show poorer agreement with experimental coupling values than those predicted from X-ray structures of other forms of the protein. Indeed the sum of the squared pair-wise deviations between experimental and predicted DC values for the 1DMB structure is 30-70 % higher than for any other X-ray structure.

To get a crude estimate of the range of accessible conformations of MBP we repeated the CNS calculations without using any DC restraints. The sampled regions of conformational space were strongly dependent on the X-ray structure used as the starting template. Although this procedure does not sample the entire conformational space, nevertheless variations of -2° to 45° (closure), -15° to 20° (twist), and -8° to 8° (bend) were observed in the ensemble of 50 conformations. Thus, a considerable number of conformations can potentially be adopted by the protein in solution, binding of ligand notwithstanding. In this regard, there are several lines of evidence that suggest that both domains are either reasonably static or experience similar amounts of motion. First alignment parameters, A_a and R (see equation (2) below), calculated for N and C-domains separately are very similar (differences of less than 4 % for the dipolar coupling data set obtained from MBP + maltotriose; differences of less than 1 % for other dipolar data sets). Second, $\{^1\text{HN}\}$-^{15}N steady-state NOE values are very similar for residues in each of the domains in all forms of the protein (differences of less than 1.5 % between N and C-domains) and, as discussed above, are greater than 0.7 for residues in the linker regions of the molecule. Third, excellent agreement between measured and predicted DC values are obtained on a per domain basis, as indicated by calculated Q values (see above). Simulations establish that the magnitude of the differences between measured and predicted values can be completely explained

by structural noise. Finally, the fact that essentially the same domain orientations are obtained for the apo form of MBP in solution and crystal states, as well as for the maltotriose bound form, suggests strongly that domain motions, if present, do not affect the accuracy of the orientation procedure.

As a final note, we have investigated the consistency of the chemical shift-based dihedral angle restraints derived using the program TALOS[53] with the linker conformations obtained from the DC values. Structure calculations were repeated with the addition of TALOS restraints for the linker residues resulting in closure, bend and twist angles similar to those determined previously (maximal r.m.s.d values for closure, twist and bend of 0.7°, 2.2°, 0.6°) but with somewhat improved precision. In addition, the penalty functions for both the DC restraints and the simulated distance and dihedral restraints were virtually unchanged, indicating that the TALOS derived dihedral angles are fully compatible with all the input data.

Conclusion

Results from a dipolar coupling and chemical shift-based study of the apo, β-cyclodextrin and maltotriose-bound states of MBP in solution have been described. The NMR data indicates that ligand binding primarily involves changes in domain orientations, critical for interaction with the Tar and $MalFGK_2$ receptors.[5,6] Local structural changes mainly occur at the domain interface as indicated by chemical shift data. The invariance of intra-domain structure is further confirmed by the residual DC data. These couplings were used to generate models of the solution conformations of MBP by applying a quasi rigid-body optimization algorithm to X-ray structures of the protein. The domain orientations in apo and maltotriose-bound states are in good agreement with the results of X-ray studies.[9,10] In contrast, significant differences between the solution and crystalline states of the MBP/β-cyclodextrin complex are noted, likely due to packing effects in the crystal lattice. The present study demonstrates the utility of DC data for the investigation of relative domain orientation in multi-domain proteins, in particular in relation to the changes occurring upon binding of ligands.

Materials and Methods

NMR samples

Uniformly ^{15}N and ^{13}C-labeled *Escherichia coli* maltodextrin-binding protein (MBP), extensively deuterated at aliphatic and aromatic positions, was prepared as described,[34] but without selective protonation of methyl groups. The NMR studies on the ligand-free state were performed using two 500 μl samples of 1.4 mM (no phage) or 1.1 mM protein (phage), 20 mM sodium phosphate buffer (pH 7.2), 3 mM NaN_3, 0.1 mM EDTA, 50 μM Pefabloc, 10 % ^2H_2O. The aligned sample was obtained by adding Pf1 phage[40] to a concentration of ~18 mg/ml (^2H splitting of 18 Hz). Maltotriose (purity >99 %) was purchased from ICN Pharmaceuticals and was used without further purification. Two samples of maltotriose-bound MBP with and without aligning media were obtained by stepwise additions of 50 mM maltotriose solution to the ligand-free MBP samples yielding final maltotriose concentrations of 3 mM (no phage) and 4 mM (phage) and protein concentrations of 1.3 mM (no phage) and 1.0 mM (phage).

NMR spectroscopy

All NMR experiments were recorded at 37 °C on a 600 MHz Varian Inova spectrometer, except for spectra used for assignment of maltotriose-bound MBP that were recorded on a 500 MHz Varian Inova spectrometer. TROSY-modified 3D CT-HNCA, CT-HN(CO)CA, CT-HN(CA)CB and CT-HN(COCA)CB experiments (see supporting information described by Yang & Kay[54]) were used to obtain backbone and $^{13}C^{\beta}$ assignments. Acquisition and processing parameters were very similar to those described.[55–57] DC data ($^1D_{NH}$, $^1D_{NCO}$, $^1D_{COC\alpha}$, $^2D_{HNCO}$ and $^3D_{HNC\alpha}$) were obtained using 3D TROSY-HNCO-based experiments, acquired and processed in an identical manner to the experiments performed on β-cyclodextrin-loaded MBP as described.[41] One-bond $^{13}C^{\alpha}$-$^{13}C^{\beta}$ dipolar couplings ($^1D_{C\alpha C\beta}$) have been measured recently for apo-MBP using a TROSY-based HN(CO)CA 2D pulse sequence as described in detail elsewhere.[42] Briefly, the $^{13}C^{\alpha}$-$^{13}C^{\beta}$ dipolar couplings were obtained from the time modulation of cross-peak intensities in a set of 2D ^{15}N-^1HN correlated spectra, recorded both in the absence and presence of aligning media. The measurements of {^1HN}-^{15}N steady-state heteronuclear Overhauser enhancements (NOE) were performed using a TROSY-modified[58] version of the 2D pulsed-field gradient-enhanced experiment described earlier.[59] The NOE values were determined from spectra, recorded with (NOE) and without (REF) a ^1H pre-saturation period of five seconds, by calculating the cross-peak intensity ratio, $NOE = I_{NOE}/I_{REF}$. A relaxation delay of 15 seconds was used between the transients for the REF spectra, while a relaxation delay of ten seconds prior to the pre-saturation period was employed for the NOE spectra. NMR data sets were processed using the NMRPipe/NMRDraw software suite.[60]

Chemical shifts

NMR spectra were analyzed using NMRView software[61] in conjunction with auxiliary scripts written in-house. The ^1HN, ^{15}N, $^{13}C^{\alpha}$, and $^{13}C^{\beta}$ chemical shifts were independently assigned for ligand-free and maltotriose-bound MBP using well-established constant-time triple resonance methodology[55–57] developed for ^{15}N, ^{13}C, ^2H-labeled proteins. The ^{13}CO chemical shifts were assigned on the basis of the ^1HN and ^{15}N chemical shifts from 3D HNCO spectra.[62] Prior to chemical shift analysis, $^{13}C^{\alpha}/^{13}C^{\beta}$ chemical shifts were corrected for ^2H-isotope effects as described by Venters *et al.*[63] In addition, ^{15}N chemical shifts were uniformly corrected by +0.23 ppm.[64] No correction was made for ^1HN and ^{13}CO chemical shifts. The ^1HN, ^{15}N, $^{13}C^{\alpha}$, $^{13}C^{\beta}$ and ^{13}CO assignments of the apo and maltotriose-bound states of MBP have been deposited in the BioMagResBank (URL

http://www.bmrb.wisc.edu). Backbone dihedral angles ϕ and ψ were predicted from ^{15}N, $^{13}C^{\alpha}$, $^{13}C^{\beta}$ and ^{13}CO chemical shifts using the TALOS program.[53] The chemical shifts of MBP in complex with β-cyclodextrin[34] were removed from the data base prior to the predictions. The error used for each dihedral angle restraint was set to the standard deviation multiplied by 2 or to a minimum value of 15°.

The combined chemical shift change of a particular residue upon ligand-binding was calculated as:

$$\Delta\delta_{tot} = \sqrt{(w_N\Delta\delta_N)^2 + (w_{C\alpha}\Delta\delta_{C\alpha})^2 + (w_{C\beta}\Delta\delta_{C\beta})^2 + (w_{CO}\Delta\delta_{CO})^2}$$

where w_i denotes the weight factor of nucleus i. The weight factors were determined from the ratio of the average variances,[65,66] $\langle\sigma_\delta\rangle_{HN}/\langle\sigma_\delta\rangle_i$, of the ^1HN shifts and the chemical shifts of nucleus type i as observed for the 20 common amino acids in proteins using the BioMagResBank chemical shift database; $w_{HN} = 1$, $w_N = 0.154$, $w_{C\alpha} = 0.276$ and $w_{CO} = 0.341$ (F. Mulder, personal communication), and assuming that $w_{C\alpha} = w_{C\beta}$. Since ^1H chemical shifts are more sensitive to surrounding local magnetic fields than ^{13}C and ^{15}N chemical shifts (for example, to altered distances to aromatic rings[67]), ^1HN chemical shifts were not taken into account in the calculation so that the value of $\Delta\delta_{tot}$ reflects principally changes in backbone ϕ/ψ angles.

Dipolar couplings

The $^1D_{NH}$, $^1D_{NCO}$, $^1D_{COC\alpha}$, $^2D_{HNCO}$ and $^3D_{HNC\alpha}$ values were measured for apo and maltotriose-bound MBP from 3D TROSY-HNCO spectra[41] which were analyzed using the PIPP/CAPP suite of programs.[68] The corresponding DC data from the β-cyclodextrin-bound state of MBP have been reported.[41] Only the one-bond dipolar couplings were used for the structural studies of the ligand-free and the two bound states of MBP because of their better precision and accuracy. The number of $^1D_{NH}$, $^1D_{NCO}$, and $^1D_{COC\alpha}$ values obtained were 310, 294, and 299 (apo-MBP); 278, 260 and 275 (β-cyclodextrin-bound MBP); and 312, 300 and 296 (maltotriose-bound MBP). In addition, 165 $^1D_{C\alpha C\beta}$ values were available for apo-MBP.[42] Uncertainties were obtained from the pair-wise r.m.s.d. of DC data from repeat experiments:[41] 0.2 Hz ($^1D_{NCO}$) and 0.7 Hz ($^1D_{NH}$, $^1D_{COC\alpha}$). Residue-specific errors of the $^1D_{C\alpha C\beta}$ values have been estimated previously (average error ~0.15 Hz).[42]

Alignment parameters, A_a, R, and the three Euler angles {α, β, δ}, were obtained by optimizing the agreement between the experimental DC data and DCs predicted from a given 3D structure using the in-house software Conformist 1.0.[25] Predicted DC values are calculated from the coordinates of the 3D structure using the following relationship:[69,70]

$$D_{ij} = D_{ij}^0 A_a S\left[(3\cos^2\theta - 1) + \frac{3}{2}R\sin^2\theta\cos 2\phi\right] \quad (2)$$

where $D_{ij}^0 = -(1/2\pi)(\mu_0/4\pi)\gamma_i\gamma_j\hbar\langle r_{ij}^{-3}\rangle$ is the dipolar interaction constant, r_{ij} is distance between nuclei i and j, γ_i is the gyromagnetic ratio of nucleus i, S is the order parameter that reflects averaging due to fast local dynamics and A_a and R are the axial and rhombic components of the alignment tensor, respectively. The polar angles {θ, φ} describe the orientation of the dipolar vector with respect to the alignment frame. The Euler angles {α, β, γ} describe the orientation of the alignment tensor principal axes with respect to the PDB frame.

Domain orientations and CNS calculations

All vectors and rotations are described with respect to the reference molecular frame provided by the 1OMP coordinate file of ligand-free MBP.[10] In the analyses of domain orientations in any structure, the C-domain is first superimposed onto the 1OMP C-domain using MOLMOL.[71] The relative domain orientations are then described as a series of rigid-body rotations about the closure, twist and bend axes required to superimpose the 1OMP N-domain onto the N-domain of the investigated structure.[25] The polar angles of the closure, twist and bend axes with respect to the 1OMP molecular frame are {109°, 124°}, {159°, 279°}, {82°, 212°}.

Models of the solution conformations of MBP in the apo, β-cyclodextrin-bound and maltotriose-bound states were generated using an algorithm implemented within the CNS software package developed for macromolecular structure calculation[32] as very recently described in conformational studies of T4 lysozyme.[45] Briefly, the method reorients the domains of an X-ray crystal structure guided by the experimentally determined DC values. For each of the three states of MBP studied by NMR, ten solution conformations were calculated using each of the five X-ray structures of MBP listed in Table 1 as the starting structure. DC restraints were not included for residues in ill-defined regions of the crystal structures. Specifically, DC restraints were omitted for residues for which the average backbone *B*-factor exceeded 1.7 times the average *B*-factor of all backbone heavy atoms in the protein. In this manner, residues 1-5, 25-34, 41, 50-55, 80-84, 100-101, 171-175, 185, 352-354, and 369-370 were identified as ill-defined in at least one of the crystal structures.

Direct refinement of protein structures using residual DC data can result in largely unphysical adjustments of individual bond orientations or movement of peptide planes without reorienting domains. To alleviate this problem, an extensive set of synthetic intra-domain restraints were generated from the X-ray coordinates of each starting structure. The synthetic intra-domain restraints included (1) distances involving all HN-HN and N-N pairs separated by less than 15 Å; and (2) backbone dihedral angles, ψ and φ. No inter-domain distance restraints were used at any stage. Prior to extraction of distances and angles, standard protonation and refinement protocols were applied to each crystal structure.[32] Experimental DC NMR restraints were included for the entire protein and, in particular, for the linker regions, residues 110-113, 259-263 and 310-315, in order to steer these residues towards the average solution conformation. The number of DC restraints available for linker residues was 43 (959), 37 (725) and 40 (818) for the apo, β-cyclodextrin-bound, and maltotriose-bound states of MBP, respectively, with the number in parenthesis indicating the total number of DC values employed in the calculations. All DC values and errors in the CNS input tables were scaled with respect to the ^1HN-^{15}N couplings to enable the use of a single force constant. TALOS restraints on the dihedral backbone angles, ψ and φ, available for 10 (apo), 10 (β-cyclodextrin), and 8 residues (maltotriose) out of the 15 linker amino-acids, were incorporated in some of the calculations.

Experimental residual DC data were included in structure calculations using the CNS module described by Clore and co-workers.[72] In a preliminary step, the rigid-body approach for domain reorientation described by Skrynnikov *et al*.[25] (Conformist1.0) was used to optimize the alignment parameters: $D_a = 15.81$ Hz and $R = 0.25$ (apo); $D_a = 16.10$ Hz and $R = 0.18$ (β-cyclodextrin); and $D_a = 15.77$ Hz and $R = 0.43$ (maltotriose), where $D_a = D^0_{NH}A_aS$, *cf*. equation (2). An artificial tetra-atomic molecule representing the estimated set of alignment axes was placed 200 Å away from the origin. The orientation of this pseudo-molecule was allowed to float during the torsion angle dynamics period of the refinement protocol. In the structure calculation protocol implemented,[45] low-temperature torsional angle dynamics is first performed[73,74] with the system cooled from 200 to 0 K in steps of 5 K. At each temperature step 15 ps of molecular dynamics are recorded with a time-step of 3 fs. The force constant for DC restraints is ramped from 0.05 to 0.5 kcal/(mol Hz^2).[74] Synthetic distance restraints are enforced by a parabolic potential with a force constant of 200 kcal/(mol Å^2) and a very narrow flat region (±0.01 Å). Similarly, intra-domain backbone dihedral angles are restrained using a steep parabolic potential (5000 kcal/(mol rad^2), ±0.1°). In addition, the force constant for the Van der Waals interactions is ramped from 0.1 to 1 kcal/(mol Å^2). The tight restraints imposed ensure that there is little change in intra-domain structure between the starting X-ray and final solution conformations. Maximum deviations in φ and ψ angles of less than 4° are obtained with differences on average of less than 1°. After the low-temperature simulated annealing stage described above, the structure is refined using ten cycles of conjugate gradient minimization with the force constants set to 150 kcal/(mol Å^2) and 600 kcal/(mol rad^2) for synthetic distance and dihedral angle restraints, respectively.

Acknowledgments

This work was supported by a grant from the Medical Research Council of Canada. We thank Drs Frans Mulder, Daiwen Yang and Wing-Yiu Choy for helpful discussions and assistance. J.E. was a recipient of a post-doctoral fellowship from the Swedish Foundation for International Cooperation in Research and Higher Education (STINT), V.T. holds a Rothschild post-doctoral fellowship, and N.R.S is supported by a Medical Research Council of Canada Centennial Fellowship. L.E.K is an International Howard Hughes Research Scholar.

References

1. Quiocho, F. A. & Ledvina, P. S. (1996). Atomic structure and specificity of bacterial periplasmic receptors for active transport and chemotaxis: variation of common themes. *Mol. Microbiol.* **20**, 17-25.
2. Kellermann, O. & Szmelcman, S. (1974). Active transport of maltose in *Escherichia coli* K12. Involvement of a ''periplasmic'' maltose binding protein. *Eur. J. Biochem.* **47**, 139-149.
3. Miller, D. M., Olson, J. S., Pflugrath, J. W. & Quiocho, F. A. (1983). Rates of ligand binding to periplasmic binding proteins involved in bacterial transport and chemotaxis. *J. Biol. Chem.* **258**, 13193-13198.
4. Boos, W. & Shuman, H. (1998). Maltose/maltodextrin system of *Escherichia coli*: transport, metabolism, and regulation. *Microbiol. Mol. Biol. Rev.* **62**, 204-229.
5. Davidson, A. L., Shuman, H. A. & Nikaido, H. (1992). Mechanism of maltose transport in *Escherichia coli*: transmembrane signaling by periplasmic binding proteins. *Proc. Natl Acad. Sci. USA,* **89**, 2360-2364.
6. Dahl, M. K. & Manson, M. D. (1985). Interspecific reconstitution of maltose transport and chemotaxis in *Escherichia coli* with maltose-binding protein from various enteric bacteria. *J. Bacteriol.* **164**, 1057-1063.
7. Mowbray, S. L. & Sandgren, M. O. (1998). Chemotaxis receptors: a progress report on structure and function. *J. Struct. Biol.* **124**, 257-275.
8. Spurlino, J. C., Lu, G. Y. & Quiocho, F. A. (1991). The 2.3 Å resolution structure of the maltose- or maltodextrin-binding protein, a primary receptor of bacterial active transport and chemotaxis. *J. Biol. Chem.* **266**, 5202-5219.
9. Quiocho, F., Spurlino, J. & Rodseth, L. (1997). Extensive features of tight oligosaccharide binding revealed in high-resolution structures of the maltodextrin transport/chemosensory receptor. *Structure,* **5**, 997-1015.
10. Sharff, A. J., Rodseth, L. E., Spurlino, J. C. & Quiocho, F. A. (1992). Crystallographic evidence of a large ligand-induced hinge-twist motion between the two domains of the maltodextrin binding protein involved in active transport and chemotaxis. *Biochemistry,* **31**, 10657-10663.
11. Gilardi, G., Zhou, L. Q., Hibbert, L. & Cass, A. E. (1994). Engineering the maltose binding protein for reagentless fluorescence sensing. *Anal. Chem.* **66**, 3840-3847.
12. Gilardi, G., Mei, G., Rosato, N., Agro, A. F. & Cass, A. E. (1997). Spectroscopic properties of an engineered maltose binding protein. *Protein Eng.* **10**, 479-486.
13. Novokhatny, V. & Ingham, K. (1997). Thermodynamics of maltose binding protein unfolding. *Protein Sci.* **6**, 141-146.
14. Hor, L. I. & Shuman, H. A. (1993). Genetic analysis of periplasmic binding protein dependent transport in *Escherichia coli*. Each lobe of maltose-binding protein interacts with a different subunit of the MalFGK2 membrane transport complex. *J. Mol. Biol.* **233**, 659-670.
15. Treptow, N. A. & Shuman, H. A. (1988). Allele-specific malE mutations that restore interactions between maltose-binding protein and the inner-membrane components of the maltose transport system. *J. Mol. Biol.* **202**, 809-822.
16. Zhang, Y., Mannering, D. E., Davidson, A. L., Yao, N. & Manson, M. D. (1996). Maltose-binding protein containing an interdomain disulfide bridge confers a dominant-negative phenotype for transport and chemotaxis. *J. Biol. Chem.* **271**, 17881-17889.
17. Ferenci, T. & Boos, W. (1980). The role of the *Escherichia coli* lambda receptor in the transport of maltose and maltodextrins. *J. Supramol. Struct.* **13**, 101-116.
18. Ferenci, T., Muir, M., Lee, K. S. & Maris, D. (1986). Substrate specificity of the *Escherichia coli* maltodextrin transport system and its component proteins. *Biochim. Biophys. Acta,* **860**, 44-50.
19. Gehring, K., Williams, P. G., Pelton, J. G., Morimoto, H. & Wemmer, D. E. (1991). Tritium NMR

spectroscopy of ligand binding to maltose-binding protein. *Biochemistry,* **30**, 5524-5531.
20. Gehring, K., Zhang, X., Hall, J., Nikaido, H. & Wemmer, D. E. (1998). An NMR study of ligand binding by maltodextrin binding protein. *Biochem. Cell. Biol.* **76**, 189-197.
21. Hall, J. A., Gehring, K. & Nikaido, H. (1997). Two modes of ligand binding in maltose-binding protein of *Escherichia coli*. Correlation with the structure of ligands and the structure of binding protein. *J. Biol. Chem.* **272**, 17605-17609.
22. Hall, J. A., Ganesan, A. K., Chen, J. & Nikaido, H. (1997). Two modes of ligand binding in maltose-binding protein of *Escherichia coli*. Functional significance in active transport. *J. Biol. Chem.* **272**, 17615-17622.
23. Hall, J. A., Thorgeirsson, T. E., Liu, J., Shin, Y. K. & Nikaido, H. (1997). Two modes of ligand binding in maltose-binding protein of *Escherichia coli*. Electron paramagnetic resonance study of ligand-induced global conformational changes by site-directed spin labeling. *J. Biol. Chem.* **272**, 17610-17614.
24. Sharff, A. J., Rodseth, L. E. & Quiocho, F. A. (1993). Refined 1.8-Å structure reveals the mode of binding of β-cyclodextrin to the maltodextrin binding protein. *Biochemistry,* **32**, 10553-10559.
25. Skrynnikov, N. R., Goto, N. K., Yang, D., Choy, W. Y., Tolman, J. R., Mueller, G. A. & Kay, L. E. (2000). Orienting domains in proteins using dipolar couplings measured by liquid-state NMR: differences in solution and crystal forms of maltodextrin binding protein loaded with β-cyclodextrin. *J. Mol. Biol.* **295**, 1265-1273.
26. Mueller, G. A., Choy, W. Y., Yang, D., Forman-Kay, J. D., Venters, R. A. & Kay, L. E. (2000). Global folds of proteins with low densities of NOEs using residual dipolar couplings: application to the 370-residue maltodextrin-binding protein. *J. Mol. Biol.* **300**, 197-212.
27. Gardner, K. H. & Kay, L. E. (1998). The use of ^{2}H, ^{13}C, ^{15}N multidimensional NMR to study the structure and dynamics of proteins. *Annu. Rev. Biophys. Biomol. Struct.* **27**, 357-406.
28. Farmer, B. T. & Venters, R. A. (1998). NMR of perdeuterated large proteins. In *Biological Magnetic Resonance* (Krishna, N. R. & Berliner, L. J., eds), vol. 16, pp. 75-120, Kluwer Academic/Plenum Publishers, New York.
29. Tjandra, N., Omichinski, J. G., Gronenborn, A. M., Clore, G. M. & Bax, A. (1997). Using dipolar ^{1}H-^{15}N and ^{1}H-^{13}C couplings in the structure determination of magnetically oriented macromolecules in solution. *Nature Struct. Biol.* **4**, 732-738.
30. Fischer, M. W., Losonczi, J. A., Weaver, J. L. & Prestegard, J. H. (1999). Domain orientation and dynamics in multidomain proteins from residual dipolar couplings. *Biochemistry,* **38**, 9013-9022.
31. Clore, G. M. (2000). Accurate and rapid docking of protein-protein complexes on the basis of internuclear Overhauser enhancement data and dipolar couplings by rigid body minimization. *Proc. Natl Acad. Sci. USA,* **97**, 9021-9025.
32. Brunger, A. T., Adams, P. D., Clore, G. M., DeLano, W. L., Gros, P., Grosse-Kunstleve, R. W., Jiang, J. S., Kuszewski, J., Nilges, M., Pannu, N. S., Read, R. J., Rice, L. M., Simonson, T. & Warren, G. L. (1998). Crystallography & NMR system: a new software suite for macromolecular structure determination. *Acta Crystallog. sect. D,* **54**, 905-921.
33. Bax, A. (1994). Multidimensional nuclear magnetic resonance methods for protein studies. *Curr. Opin. Struct. Biol.* **4**, 738-744.
34. Gardner, K. H., Zhang, X., Gehring, K. & Kay, L. E. (1998). Solution NMR studies of a 42 kDa *E. coli* maltose binding protein/β cyclodextrin complex: chemical shift assignments and analysis. *J. Am. Chem. Soc.* **120**, 11738-11748.
35. Wishart, D. S., Bigam, C. G., Holm, A., Hodges, R. S. & Sykes, B. D. (1995). ^{1}H, ^{13}C and ^{15}N random coil NMR chemical shifts of the common amino acids. I. Investigations of nearest-neighbor effects. *J. Biomol. NMR,* **5**, 67-81.
36. Hwang, P. M., Skrynnikov, N. R. & Kay, L. E. (2001). Domain orientation in β-cyclodextrin-loaded maltose binding protein: diffusion anisotropy measurements confirm the results of a dipolar coupling study. J. Biomol. NMR, in the press.
37. Kay, L. E., Muhandiram, D. R., Wolf, G., Shoelson, S. E. & Forman-Kay, J. D. (1998). Correlation between binding and dynamics at SH2 domain interfaces. *Nature Struct. Biol.* **5**, 156-163.
38. Zhang, Y., Gardina, P. J., Kuebler, A. S., Kang, H. S., Christopher, J. A. & Manson, M. D. (1999). Model of maltose-binding protein/chemoreceptor complex supports intrasubunit signaling mechanism. *Proc. Natl Acad. Sci. USA,* **96**, 939-944.
39. Tolman, J. R., Flanagan, J. M., Kennedy, M. A. & Prestegard, J. H. (1995). Nuclear magnetic dipole interactions in field-oriented proteins: information for structure determination in solution. *Proc. Natl Acad. Sci. USA,* **92**, 9279-9283.
40. Hansen, M. R., Mueller, L. & Pardi, A. (1998). Tunable alignment of macromolecules by filamentous phage yields dipolar coupling interactions. *Nature Struct. Biol.* **5**, 1065-1074.
41. Yang, D., Venters, R. A., Mueller, G. A., Choy, W. Y. & Kay, L. E. (1999). TROSY-based HNCO pulse sequences for the measurement of ^{1}HN-^{15}N, ^{15}N-^{13}CO, ^{1}HN-^{13}CO, ^{13}CO-$^{13}C^{\alpha}$ dipolar couplings in ^{15}N, ^{13}C, ^{2}H-labeled proteins. *J. Biomol. NMR,* **14**, 333-343.
42. Evenäs, J., Mittermaier, A., Yang, D. & Kay, L. E. (2001). Measurement of $^{13}C^{\alpha}$-$^{13}C^{\beta}$ dipolar couplings in ^{15}N,^{13}C,^{2}H-labeled proteins: application to domain orientation in maltose binding protein. *J. Am. Chem. Soc.* **123**, 2858-2864.
43. Hayward, S., Kitao, A. & Berendsen, H. J. C. (1997). Model-free methods of analyzing domain motions in proteins from simulation: a comparison of normal mode analysis and molecular dynamics simulation of lysozyme. *Proteins: Struct. Funct. Genet.* **27**, 425-437.
44. Van Alten, D. M. F., Conn, D. A., De Groot, B. L., Findlay, J. B. C. & Berendsen, H. J. C. (1997). Protein dynamics derived from clusters of crystal structures. *Biophys. J.* **73**, 2891-2896.
45. Goto, N. K., Skrynnikov, N. R., Dahlquist, F. W. & Kay, L. E. (2001). What is the average conformation of bacteriophage T4 lysozyme in solution? A domain orientation study using dipolar couplings measured by solution NMR. *J. Mol. Biol.* **308**, 745-764.
46. Maiorov, V. & Abagyan, R. (1997). A new method for modeling large-scale rearrangements of protein domains. *Proteins: Struct. Funct. Genet.* **27**, 410-424.
47. Brüschweiler, R., Liao, X. & Wright, P. E. (1995). Long-range motional restrictions in a multidomain

zinc-finger protein from anisotropic tumbling. *Science,* **268**, 886-889.
48. Björkman, A. J. & Mowbray, S. L. (1998). Multiple open forms of ribose-binding protein trace the path of its conformational change. *J. Mol. Biol.* **279**, 651-664.
49. Flocco, M. M. & Mowbray, S. L. (1994). The 1.9 Å X-ray structure of a closed unliganded form of the periplasmic glucose/galactose receptor from Salmonella typhimurium. *J. Biol. Chem.* **269**, 8931-8936.
50. Zhang, X.-J., Wozniak, J. A. & Matthews, B. W. (1995). Protein flexibility and adaptability seen in 25 crystal forms of T4 lysozyme. *J. Mol. Biol.* **250**, 527-552.
51. Laskowski, R. A., Rullman, J. A. C., MacArthur, M. W., Kaptein, R. & Thornton, J. M. (1998). AQUA and PROCHECK-NMR: programs for checking the quality of protein structures solved by NMR. *J. Biomol. NMR,* **8**, 477-486.
52. Ottiger, M. & Bax, A. (1999). Bicelle-based liquid crystals for NMR-measurement of dipolar couplings at acidic and basic pH values. *J. Biomol. NMR,* **13**, 187-191.
53. Cornilescu, G., Delaglio, F. & Bax, A. (1999). Protein backbone angle restraints from searching a database for chemical shift and sequence homology. *J. Biomol. NMR,* **13**, 289-302.
54. Yang, D. & Kay, L. E. (1999). TROSY triple resonance four-dimensional NMR spectroscopy of a 46 ns tumbling protein. *J. Am. Chem. Soc.* **121**, 2571-2575.
55. Yamazaki, T., Lee, W., Arrowsmith, C. H., Muhandiram, D. R. & Kay, L. E. (1994). A suite of triple resonance NMR experiments for the backbone assignment of ^{15}N, ^{13}C, ^{2}H labeled proteins with high sensitivity. *J. Am. Chem. Soc.* **116**, 11655-11666.
56. Shan, X., Gardner, K. H., Muhandiram, D. R., Rao, N. S., Arrowsmith, C. H. & Kay, L. E. (1996). Assignment of ^{15}N, ^{13}Cα, ^{13}Cβ and HN resonances in an ^{15}N, ^{13}C, ^{2}H labeled 64 kDa trp repressor-operator complex using triple resonance NMR spectroscopy and ^{2}H-decoupling. *J. Am. Chem. Soc.* **118**, 6570-6579.
57. Yamazaki, T., Lee, W., Revington, M., Mattiello, D. L., Dahlquist, F. W., Arrowsmith, C. H. & Kay, L. E. (1994). An HNCA pulse scheme for the backbone assignment of ^{15}N, ^{13}C, ^{2}H labeled proteins: application to a 37 kDa trp repressor-DNA complex. *J. Am. Chem. Soc.* **116**, 6464-6465.
58. Pervushin, K., Riek, R., Wider, G. & Wüthrich, K. (1997). Attenuated T_2 relaxation by mutual cancellation of dipole-dipole coupling and chemical shift anisotropy indicates an avenue to NMR structures of very large biological macromolecules in solution. *Proc. Natl Acad. Sci. USA,* **94**, 12366-12371.
59. Farrow, N. A., Muhandiram, R., Singer, A. U., Pascal, S. M., Kay, C. M., Gish, G., Shoelson, S. E., Pawson, T., Forman-Kay, J. D. & Kay, L. E. (1994). Backbone dynamics of a free and phosphopeptide-complexed src homology 2 domain studied by ^{15}N NMR relaxation. *Biochemistry,* **33**, 5984-6003.
60. Delaglio, F., Grzesiek, S., Vuister, G. W., Zhu, G., Pfeifer, J. & Bax, A. (1995). NMRPipe: a multidimensional spectral processing system based on UNIX pipes. *J. Biomol. NMR,* **6**, 277-293.
61. Johnson, B. A. & Blevins, R. A. (1994). NMRView: a computer program for the visualization and analysis of NMR data. *J. Biomol. NMR,* **4**, 603-614.
62. Kay, L. E., Xu, G. Y. & Yamazaki, T. (1994). Enhanced-sensitivity triple-resonance spectroscopy with minimal H_2O saturation. *J. Magn. Reson. ser. A,* **109**, 129-133.
63. Venters, R. A., Farmer, B. T., Fierke, C. A. & Spicer, L. D. (1996). Characterizing the use of perdeuteration in NMR studies of large proteins: ^{13}C, ^{15}N and ^{1}H assignments of human carbonic anhydrase II. *J. Mol. Biol.* **264**, 1101-1116.
64. Gardner, K. H., Rosen, M. K. & Kay, L. E. (1997). Global folds of highly deuterated, methyl protonated proteins by multidimensional NMR. *Biochemistry,* **36**, 1389-1401.
65. Mulder, F. A. A. (1998). NMR relaxation studies of protein dynamics in solution. Doctoral thesis, Utrecht University, The Netherlands.
66. Mulder, F. A. A., Schipper, D., Bott, R. & Boelens, R. (1999). Altered flexibility in the substrate-binding site of related native and engineered high-alkaline *Bacillus* subtilisins. *J. Mol. Biol.* **292**, 111-123.
67. Ishima, R., Wingfield, P. T., Stahl, S. J., Kaufman, J. D. & Torchia, D. A. (1998). Using amide ^{1}H and ^{15}N transverse relaxation to detect millisecond timescale motions in perdeuterated proteins: application to HIV-1 protease. *J. Am. Chem. Soc.* **120**, 10534-10542.
68. Garrett, D. S., Powers, R., Gronenborn, A. M. & Clore, G. M. (1991). A common sense approach to peak picking in two-, three-, and four-dimensional spectra using automatic computer analysis of contour diagrams. *J. Magn. Reson.* **95**, 214-220.
69. Bastiaan, E. W., MacLean, C., van Zijl, P. C. M. & Bothner-By, A. A. (1987). High resolution NMR of liquids and gases: effects of magentic-field-induced molecular alignment. *Annu. Rep. NMR Spectrosc.* **9**, 35-77.
70. Tjandra, N. & Bax, A. (1997). Direct measurement of distances and angles in biomolecules by NMR in a dilute liquid crystalline medium. *Science,* **278**, 1111-1114.
71. Koradi, R., Billeter, M. & Wüthrich, K. (1996). MOLMOL: a program for display and analysis of macromolecular structures. *J. Mol. Graph.* **14**, 51-55.
72. Clore, G. M., Gronenborn, A. M. & Tjandra, N. (1998). Direct structure refinement against residual dipolar couplings in the presence of rhombicity of unknown magnitude. *J. Magn. Reson.* **131**, 159-162.
73. Stein, E. G., Rice, L. M. & Brunger, A. T. (1997). Torsion-angle molecular dynamics as a new efficient tool for NMR structure calculation. *J. Magn. Reson.* **124**, 154-164.
74. Chou, J. J., Li, S. & Bax, A. (2000). Study of conformational rearrangement and refinement of structural homology models by the use of heteronuclear dipolar couplings. *J. Biomol. NMR,* **18**, 217-227.

Edited by P. E. Wright

(Received 22 February 2001; received in revised form 11 April 2001; accepted 17 April 2001)